

Robot-Assisted Rapid Prototyping for Ice Structures

Eric Barnett, Jorge Angeles, Damiano Pasini

Department of Mechanical Engineering, McGill University
Montreal, Quebec H3A 2K6, Canada

ebarnett@cim.mcgill.ca, angeles@cim.mcgill.ca, damiano.pasini@mcgill.ca

Pieter Sijpkens

School of Architecture, McGill University
Montreal, Quebec H3A 2K6, Canada

pieter.sijpkens@mcgill.ca

Abstract—Ice has long been used by humankind for utilitarian purposes, and more recently for artistic and entertainment purposes. Nowadays, the field of ice construction is becoming more commercially relevant, with increased interest in ice modeling at the small scale, and in ice tourism, specifically ice hotels at the large scale. As a result, there is a market for automating ice construction, and building detailed structures that would otherwise require a significant amount of manual work. To address this demand, the authors are currently developing experimental robotic systems for building ice structures: the Fab@home, for building small-scale structures, and the Adept Cobra 600 robot, for building medium-scale structures. Further software and hardware development is needed for the Cobra, since it was not designed for rapid prototyping, and certainly not for rapid prototyping using ice as the working material. The authors have designed and built fluid delivery systems for each machine to permit the use of water as the building material. A signal-processing subsystem permits control of the water-delivery flow rate and synchronization with the robot motion. Additionally, we have developed a slicing algorithm to generate toolpaths for the Cobra using stereolithography (STL) files as the input. We also intend to develop a larger robotic system for producing ice sculptures and buildings at the architectural scale.

Index Terms—rapid prototyping, ice structures.

I. INTRODUCTION

Practical ice structures such as ice roads and igloos are critical for winter survival in Arctic areas. Moreover, recreational structures such as ice sculptures and hotels have become more and more popular in recent years. Traditionally, ice structures have been built manually, making them labor-intensive and costly. However, in the past two decades, CNC ice sculpting has become quite popular. Two of the larger companies currently working in this field are Ice Sculptures Ltd. based in Grand Rapids, MI,¹ and Ice Culture Inc. based in Hensall, Ontario, Canada.²

In this paper, we report on the development of two robot-assisted Rapid Prototyping (RP) systems for ice construction. RP is a Solid Freeform Fabrication (SFF) technique [1], which means that solid parts are built by material deposition. No specific tooling is required for RP, as in traditional manufacturing techniques such as milling and drilling, which remove material. RP is a SFF technique that is often used in industry to produce prototypes quickly and at low cost. RP with ice has additional advantages, namely, further reduced cost, small environmental impact, and high part accuracy and surface finish.

Sui and Leu developed a Rapid Freeze Prototyping (RFP) system consisting of a valve/nozzle water delivery system positioned by stepper-motor driven axes [2], [3]. They also conducted a theoretical and numerical analysis of their system parameters [4]–[6].

Our initial objective is to develop a small-scale (200 × 200 × 100 mm) system similar to that used by Sui and Leu, capable of building a brandy glass out of ice. Our next objective is to develop a faster, more accurate, and more robust system that can build medium-scale (300 × 300 × 200 mm) sculpted objects by retrofitting an Adept Cobra 600 robot.

II. THE FAB@HOME RAPID PROTOTYPING SYSTEM

The Fab@home (FAH) desktop Rapid Prototyping machine, which has the architecture of a three-axis Cartesian robot, was selected for the development of a small-scale RFP system. This machine can be purchased as a kit or as separate parts, using a bill of materials available online. The FAH is designed to build structures layer by layer using a screw-driven syringe deposition system. Colloidal materials such as silicone, epoxy, and frosting work well with this system because they hold their shape after being extruded through the syringe nozzle. The FAH connects to a PC through the USB interface, and resorts to software that can import stereolithography (STL) files, generate toolpaths, and communicate with the FAH microcontroller during the construction of a part. While the FAH system has many of the necessary elements for RFP, several modifications are essential to allow for the use of water as the deposition material.

The FAH website³ contains all documentation and software necessary for assembling and using the FAH in the initial configuration. The configuration of the FAH after modification for building ice structures is shown in Fig. 1.

A. The Fab@Home, Modified for Building Ice Structures

The syringe deposition system used by the FAH in its initial configuration is unsuitable for depositing water to form ice in a freezer maintained at -20°C because water cannot be extruded; water accumulates at the nozzle tip and eventually drips onto the build surface. Large drops will even form with a nozzle diameter of only 0.25 mm. However, if contact between the built surface and the drop forming at the nozzle can be maintained, a continuous line of water

¹<http://machinedesign.com/article/nc-router-shapes-ice-art-0217>

²<http://www.iceculture.com/main.cfm?id=5A166F80-1372-5A65-3BEEC7256C83B62C>

³http://fabathome.org/wiki/index.php?title=Main_Page

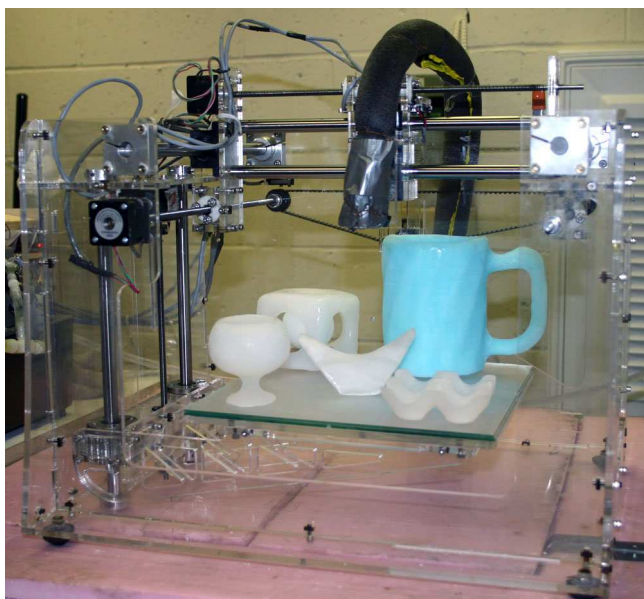


Fig. 1. The FAH rapid prototyping machine modified for building ice structures

can be deposited. Maintaining this contact requires setting the clearance between the nozzle tip and the built surface to approximately 0.15 ± 0.10 mm, a difficult task to accomplish for the whole built surface, which measures approximately $200 \text{ mm} \times 200 \text{ mm}$. Also, all errors in the system become magnified as more and more layers are deposited. As a result, structures can only be built reliably a few millimeters high.

The FAH is modified as follows to permit the use of ice as the building material: first, the screw-driven syringe system is replaced by a valve-nozzle system manufactured by the Lee Company,⁴ delivering water under pressure. This valve-nozzle system was also used by Leu and Sui in a similar experimental setup [3], [5]. A water pump is used to create pressure in the range required by the valve.

As the signal used to control the syringe motor is not suitable for the valve-nozzle system, a BasicStamp microcontroller is used to poll the syringe control signal output by the FAH microcontroller and output a new valve control signal.

Further modifications allow the FAH to operate properly in the -20°C environment of the freezer. Printed circuit boards are removed from the FAH structure and installed outside the freezer with the other control components, as shown in Fig. 2. Inside the freezer, the water lines and valve/nozzle are insulated with pipe insulation and heated with temperature-controlled resistance heating rope.

B. The Signal Conversion System

The signal used by the FAH to control the syringe deposition is a 3.3V TTL signal with a frequency of approximately 1500 Hz and a duty cycle of less than 5%. The valve's spike and hold driver, shown in Fig. 2, requires a 5V TTL signal with a duty cycle of 10–50% and a frequency of 50–900 Hz.

⁴The Lee Company, Westbrook, CT: <http://www.theleeco.com>

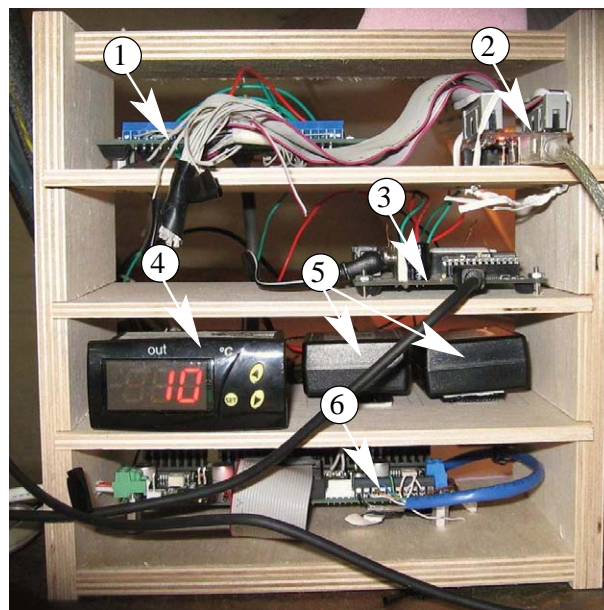


Fig. 2. The control electronics for the FAH: (1) Winford BRK25F board; (2) LPC-H2148 microcontroller; (3) Basic Stamp 2 microcontroller; (4) Omega DP-7002 temperature controller; (5) Lee Company IECX0501350A spike and hold drivers; and (6) Xylotex XS3525-8S-4 stepper motor amplifier board

In order to accomplish this signal conversion, a BasicStamp microcontroller is used to poll the FAH syringe control signal to determine if the valve should be on or off. When the valve should be on, the BasicStamp then outputs a 5V TTL control signal to the spike and hold driver at a frequency and duty cycle defined in the BasicStamp program. During each 5V TTL pulse, the spike and hold driver outputs a 24V, 0.3 ms spike to open the valve and holds it open for the duration of the pulse with a 3.5V signal. This type of control signal is used to prevent the valve from overheating.

C. The Heating System

A resistance heating coil is placed along the fluid lines and wrapped around the valve and nozzle. It is controlled by an on/off temperature controller which receives input from a thermocouple positioned to measure temperature at the nozzle tips. The setpoint of the temperature controller is 10°C , which is sufficiently low to minimize the heat transfer necessary to freeze and cool the water, but also ensure that no freezing occurs in the delivery system.

D. The Pressure Generating System

Experimentally, we have determined that a pressure of at least 30 kPa is necessary to prevent hanging drops from forming at the nozzle tips. A reservoir at an elevation of 3 m would be necessary to create this pressure, and would only provide the minimum pressure required. Instead, a pump is used to circulate water to and from a reservoir, and part of the flow in the circulating loop is diverted to the deposition valve. The flow in the loop is restricted with a needle valve to achieve a pressure range of 25 to 55 kPa at the valve.

III. THE COBRA 600 RAPID PROTOTYPING SYSTEM

The Cobra 600 system is superior to the FAH system because it is faster, more accurate, and more robust. To be true, the Cobra 600 is also around four times as expensive as the FAH. The two systems play in different leagues. The FAH can only reach a speed of 15 mm/s, while we have already had success building structures at up to 100 mm/s with the Cobra. The FAH has open-loop control, though it is programmed to find the boundaries of its workspace every few minutes to minimize positioning error. This is not necessary with the Cobra's closed-loop architecture. Finally, the FAH has a modular design: its parts are inexpensive and easily replaced. However, the parts also break much more easily, and considerable time must be spent on maintenance. Comparatively, the maintenance time necessary for the Cobra is negligible.

The fluid delivery system and the heating system used for the Cobra are almost identical to those used for the FAH. The end effector design is quite different, however. Since the Cobra is not rated for temperatures below -4°C , an extension to the distal link is necessary to allow deposition to occur deep enough in the freezer. Of course, it is also desirable to shorten the extension as much as possible to reduce dynamic loads and vibrations. Currently, we use an extension of 500 mm, and vibrations can cause horizontal error of up to 0.5 mm when the path speed is set at 50 mm/s and there are abrupt changes in direction.

A. The Signal Conversion System

The Control Interface Panel (CIP) for the Cobra has multiple output control signals available to the user. These signals function as on/off switches which can be activated from within the Adept software. In our system, one 12V output signal circuit is used to control flow through the water nozzle and another controls flow through the brine nozzle. The 12V Cobra output signal activates a function generator, which supplies a 5V TTL control signal, at a frequency of 50–450 Hz and a duty cycle of 5–50%, to the spike and hold driver described in Subsec. II-B. This system is an improvement over the FAH signal processing system because the signal conversion is accomplished with hardware components, rather than with a microcontroller.

B. Toolpath Generation

Toolpath generation is automatic using the FAH: one simply has to model a part in a CAD package, and export it to the STL format. However, we have encountered three main difficulties with the FAH software: (a) bugs in the software frequently cause models to stop building, sometimes after several successful hours; (b) simple models cannot be programmed directly; and (c) the toolpaths generated cannot be edited.

For these reasons, we have pursued two different methods for generating toolpaths for the Cobra. First, toolpaths for simple shapes can be programmed directly in Adept's V+ programming language. Second, we are developing a path-planning algorithm in Matlab that will import a STL file

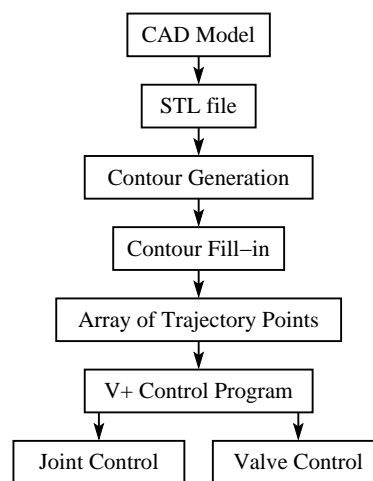


Fig. 3. Flow of information for an ice part built with the Cobra 600

and export the trajectory points that will allow the Cobra to recreate the model [7]. This algorithm implements many novel techniques, as well as other well-established techniques described in the literature [8], [9]. For both of our methods, an additional parameter is included with each trajectory point to control the valve state. Fig. 3 shows the flow of information from part modeling to path planning with our Matlab algorithm to part construction with the Cobra 600.

For our slicing algorithm, we attempt to: (a) maximize path smoothness and (b) maximize the length of paths with the valve in the on state. These types of paths help to reduce the errors described in Sec. VI, caused by abrupt changes in direction and changes in the on/off state of the valve. Two different fill-in techniques are shown in Fig. 4. The zig-zag technique shown in Fig. 4(a) is simpler, though there are frequent, abrupt changes in direction. The shrinking contour technique shown in Fig. 4(b) is preferable, because paths are much smoother. At the same time, it is more complex to program, particularly for models with multiple bounding contours per layer.

Once the toolpath trajectory has been created, two options are available for importing it to the Cobra's controller: Adept's Pathware environment or a custom V+ program. The Pathware environment is an attractive option because it is user-friendly, and has many features that ease the control of dispensing applications. However, the number of trajectory points that can be imported is very limited because all of the imported points must be stored in memory at once, and the computational capabilities of the Cobra controller are limited.⁵ Over 50 parameters are used to describe each imported point, when for our application only four are necessary to describe the location and signal state. As an example, 1000 points take several minutes to import using Pathware. Since millions of points are often necessary to approximate a CAD model using the STL format, Pathware is not feasible for our application. To overcome this problem,

⁵Our Adept C40 Compact Controller carries an AWC-II 040 Processor (25 MHz), 32MB RAM, and 128MB CompactFlash disk.

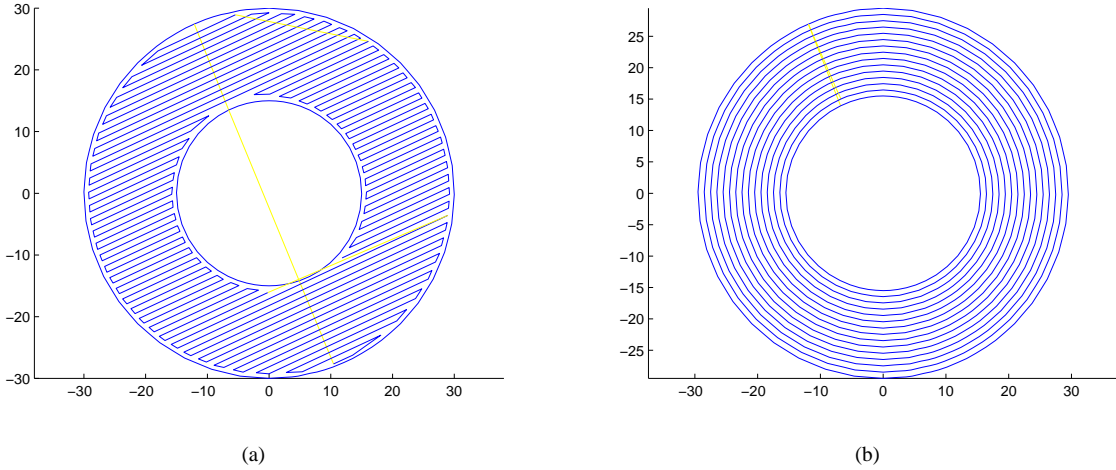


Fig. 4. STL slicing using: (a) the zig-zag technique; (b) the shrinking contour technique (Yellow lines denote non-depositing paths)

we wrote V+ programs that can import incrementally from a text file that contains only the four parameters needed for each trajectory point. Then, a minimal amount of memory is used to store points and is continually overwritten, resulting in virtually no lag during program execution.

IV. THE VALVE-NOZZLE DEPOSITION SYSTEM

Currently, the FAH has a dual-nozzle system installed, as shown in Fig. 5. The system installed for the Cobra 600 is similar, except the mount is different. One nozzle deposits water, which is used as the build material. The other nozzle deposits brine, which is used as a support structure. Deposition occurs between -20°C and -25°C .

Both fluid delivery systems were designed to be compact, well-insulated, and rigid. They must be well-insulated to prevent fluid in the liquid lines and the valves from freezing before reaching the nozzles. Rigidity is critical to maintain the horizontal distance between the nozzles constant, since this distance is used to define the nozzle offset in the FAH and Cobra software.

A mathematical model of the fluid flow through the nozzles is essential in order to predict and control the different parameters in the system. Since water can be modeled as an inviscid fluid, Bernoulli's equation applies, and for our system reduces to

$$\frac{v^2}{2} + \frac{p}{\rho} = \text{constant}, \quad (1)$$

where v is the velocity of the fluid through the nozzle, p is the system pressure, and ρ is the density. The volumetric flow rate through the nozzle can be equated with the volumetric flow rate of water being deposited to obtain

$$vN \frac{D^2}{4} = h_p v_p w_p, \quad (2)$$

where D is the nozzle diameter, N is the duty cycle, h_p is the layer height, v_p is the path velocity, and w_p is the path width. This model is quite accurate for interior paths,

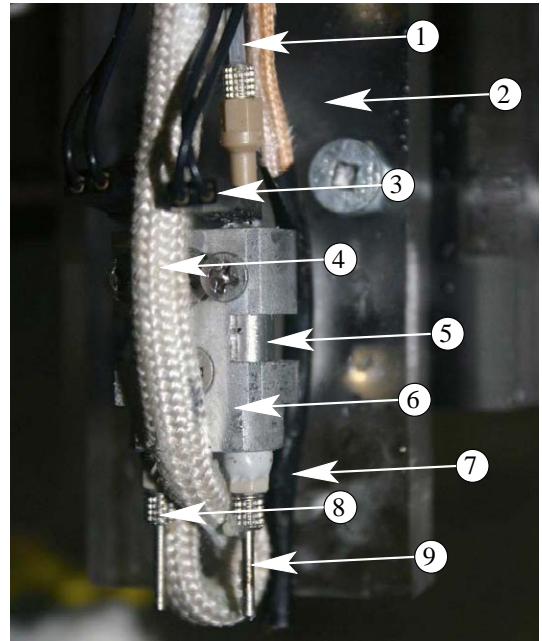


Fig. 5. The valve/nozzle assembly for the FAH: (1) Valve input line; (2) FAH mounting plate; (3) Leads from the spike and hold driver; (4) Omegalux heating rope; (5) Lee Company VHS-M/2 microdispensing valve; (6) Valve/nozzle mount; (7) Thermocouple; (8) Water nozzle; and (9) Brine nozzle

which merge together and form a solid structure. However, for paths near a part's wall, model error occurs, since the interaction of gravity and surface-tension forces leads to an undulating surface.

By combining (1) and (2) we find

$$h_p = \sqrt{\frac{2p}{\rho}} \frac{D^2 N}{4v_p w_p}. \quad (3)$$

If we substitute the parameters given in column 3 of Table I into (3), we predict $h_p = 0.39$ mm. This value is quite close to the layer height of 0.30 mm, observed experimentally.

V. THE BRINE SUPPORT MATERIAL

A support is needed to produce shapes with overhanging parts. We decided to use brine to provide the support, since the melting point of brine is slightly lower than that of water, and afterward the support structure should be safely melted away without melting the ice. The melting point of brine is obtained by using the equation for freezing point depression, valid for dilute solutions [10, p. 177]:

$$\Delta T_f = K_f m_b, \quad (4)$$

where $\Delta T_f = T_{f(\text{pure solvent})} - T_{f(\text{solution})}$, K_f is the cryoscopic constant, which depends only on the solvent, and m_b is the molality of the solution. The latter is calculated by using

$$m_b = m_{\text{solute}} i, \quad (5)$$

where m_{solute} is the moles of solute per kilogram of solvent and i is the number of ions formed by a compound in solution.

Since the molar mass for NaCl is 58.44 kg/kmol, $i = 2$ for NaCl, and $K_f = 1.86^\circ\text{C}\cdot\text{kg/mol}$ for water, a solution with 62.8 kg NaCl/m³ will have a melting point of -4°C . Similarly, since the molar mass of KCl is 74.55 kg/kmol, a solution with 80.2 kg KCl/m³ will have a melting point of -4°C .

The method used above to calculate the melting points is an idealization, since freezing is assumed to occur instantaneously. In reality, the formation of nearly pure ice crystals during freezing increases the salt concentration in the remaining solution, which gradually saturates. The eutectic point, which is the lowest melting point for the solution, occurs at saturation. At 0°C, NaCl has a solubility of 357 kg/m³, while KCl has a solubility of 280 kg/m³ [11, Table 1.68]. This means that eutectic points of -22.7°C for NaCl and -14.0°C for KCl are predicted using (4). However, in this case, (4) is only an approximation because the solutions are not dilute; the eutectic points can be found more accurately using phase diagrams or experimental measurements. Deluca and Lachman published [12] eutectic points at -21.6°C for NaCl and -11.1°C for KCl, measured experimentally.

In our system, the freezing time is approximately 10 s. It is thus expected that a dilute solution of brine placed at a temperature lower than its melting point but higher than -21.6°C for NaCl (-11.1°C for KCl) will transform to become a slightly more dilute frozen brine solution and a highly concentrated liquid brine solution. We can confirm this result experimentally, as we observed a small pool of liquid brine forming around our built models using the FAH dual-nozzle system, with 60 kg NaCl/m³ as the brine solution, and the deposition temperature as low as -23°C . This result is undesirable, since the deposited volume for the support structure is inaccurate and it does not bond to the substrate.

If KCl is used as the brine solution, however, the entire solution freezes, leading to more accurate support structures,

which help to build more accurate parts. Additionally, frozen KCl solution bonds to the substrate, preventing models from sliding.

VI. RESULTS

Several successful structures have been built with the FAH and Cobra 600 systems. Fig. 6 shows a small brandy glass made with the FAH, before and after the brine support structure is removed, while Fig. 7 shows a thin-walled structure built with the Cobra 600. Table I shows build parameter ranges as well as the parameter values for these two parts. The build times for the parts shown in Figs. 1, 6, and 7 range from five to 50 hours. Part height can increase as fast as 20 mm/h. Part height error is as low as 2% for solid structures and 5% for thin-walled structures. Solid structures have a lower error because adjacent paths merge and cancel out errors caused by asymmetry in the water jet. Horizontal error is as low as 0.5 mm. Short parts are typically much more accurate because of the relative error in the vertical direction. Surface roughness of the parts built can be as low as 0.1 mm; upon close inspection, horizontal lines can be observed on built parts.

VII. CONCLUSIONS AND FUTURE WORK

We reported on two robot-assisted rapid prototyping systems for building ice structures: one based on the Fab@home, the other on the Adept Cobra 600 robot. We have succeeded in building complex structures with both systems. In the near future, we will focus our attention on the Cobra 600 system, since it has much more potential for further development. We will also begin the transition to a large-scale system capable of building ice structures on the architectural scale.

Specifically, we plan to start building sculptures with the Cobra that require a support structure. This will require further development of our slicing algorithm and V+ programs. We would also like to increase the build speed, to complete larger structures in a reasonable amount of time.

TABLE I
BUILD PARAMETERS FOR THE FAH AND THE COBRA

Parameter	Range ^a	Ex. 1 ^b	Ex. 2 ^c
Nozzle diameter (D , mm)	0.05–0.25	0.10	0.05
Path width (w_p , mm)	0.5–1.5	1.0	0.8
Path height (h_p , mm)	0.05–0.5	0.47	0.10
Path speed (v_p , mm/s)	0–100	15	25
Gauge Pressure (p , kPa)	0–55	30	30
Valve duty cycle (N , %)	0–50	30	30
Valve frequency (Hz)	0–450	150	250
Freezer temp. ($^\circ\text{C}$)	-23	-23	-23
Water/brine temp. at nozzle tip ($^\circ\text{C}$)	0–20	10	5
KCl concentration (kg/m ³)	0–280	80	80

^a Range of values attainable with the hardware we currently have.

^b Parameters for the brandy glass shown in Fig. 6.

^c Parameters for the Koch snowflake structure shown in Fig. 7.



(a)



(b)

Fig. 6. Brandy glass: (a) with KCl brine support structure; (b) after support structure is melted in a freezer at -4°C

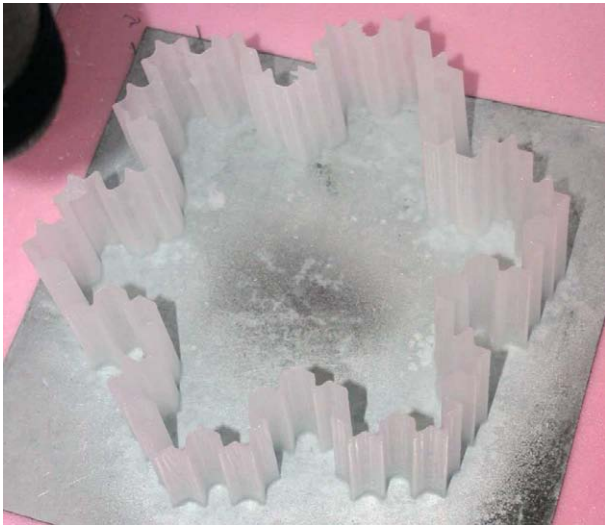


Fig. 7. Koch snowflake structure extruded: measures approximately 200 mm in diameter and 50 mm high, built with the Cobra 600 system

VIII. ACKNOWLEDGMENTS

The authors gratefully acknowledge the support received from The Social Sciences and Humanities Research Council of Canada (SSHRC), le Fonds québécois de la recherche sur la nature et les technologies, and La Fondation universitaire Pierre Arbour. Also, they would like to thank the following people who have contributed to the development of the project: David Theodore for valued discussions and administrative support; Thomas Balaban for research ideas; Thériault and Yip for assembling the FAH, Chopra, Oduncuoglu, Laughton, and Khoury for developing the fluid delivery system for the FAH; Pashley for hardware development for

both systems; and Ciat, a summer intern from Université de Paris 6, who compiled valuable information in the early stages of the project. The generous rebate received from Adept Technology is dutifully acknowledged.

REFERENCES

- [1] R. Crawford and J.J. Beaman, "Solid freeform fabrication," *IEEE Spectrum*, vol. 36, no. 2, pp. 34–43, 1999.
- [2] W. Zhang, M. Leu, Z. Yi, and Y. Yan, "Rapid freezing prototyping with water," *IEEE Spectrum*, vol. 20, pp. 139–145, 1999.
- [3] F. Bryant, G. Sui, and M. Leu, "A study on the effects of process parameters in rapid freeze prototyping," *Rapid Prototyping Journal*, vol. 9, no. 1, pp. 19–23, 2003.
- [4] G. Sui and M. Leu, "Investigation of layer thickness and surface roughness in rapid freeze prototyping," *ASME Journal of Manufacturing Science and Engineering*, vol. 125, pp. 556–563, 2003.
- [5] —, "Thermal analysis of ice walls built by rapid freeze prototyping," *ASME Journal of Manufacturing Science and Engineering*, vol. 125, pp. 824–834, 2003.
- [6] C. Feng, S. Yan, R. Zhang, and Y. Yan, "Heat transfer analysis of rapid ice prototyping process by FEM," *Materials and Design*, vol. 28, pp. 921–927, 2007.
- [7] A. Ossino and E. Barnett, "Path planning for robot-assisted rapid prototyping of ice structures," Centre for Intelligent Machines, Department of Mechanical Engineering, McGill University, Montreal, Canada, Tech. Rep. TR-CIM-09-02, January 2009.
- [8] R. Luo, Y. Pan, C. Wang, and Z. Huang, "Path planning and control of functionally graded materials for rapid tooling," in *IEEE Int. Conf. on Robotics and Automation*, Orlando, FL, May 2006, pp. 883–888.
- [9] H. Chen, N. Xi, W. Sheng, Y. Chen, A. Roche, and J. Dahl, "A general framework for automatic CAD-guided tool planning for surface manufacturing," in *IEEE Int. Conf. on Robotics and Automation*, Taipei, Taiwan, Sept. 2003, pp. 3504–3509.
- [10] P. Atkins and J. de Paula, *Atkins' Physical Chemistry, 7th Edition*. New York, NY: Oxford, 2002.
- [11] J. Speight, *Lange's Handbook of Chemistry, 16th Edition*. McGraw-Hill, 2005. [Online]. Available: http://knovel.com/web/portal/browse/display?EXT_KNOVEL_DISPLAY_bookid=1347&VerticalID=0
- [12] P. Deluca and L. Lachman, "Determination of eutectic temperatures of inorganic salts," *Lyophilization of Pharmaceuticals IV*, vol. 54, no. 10, pp. 1411–1415, 1965.